International Journal of Scientific Engineering and Applied Science (IJSEAS) – Volume-3, Issue-12, Dec 2017
ISSN: 2395-3470
www.ijseas.com

Thermal Influence on Airfoil Hydrodynamic Boundary Layer: Part 2-Test Case Results

perezruiz305@gmail.com

Miguel Toledo-Velázquez, Alfredo Pérez-Montiel, Juan Abugaber-Francis, Guilibaldo Tolentino-Eslava
Instituto Politécnico Nacional, Escuela Superior de Ingeniería Mecánica y Eléctrica. Sección de Estudios de Posgrado e Investigación. Laboratorio de Ingeniería Térmica e Hidráulica Aplicada (LABINTHAP). Unidad Profesional "Adolfo López Mateos", Edif. 5, 3er piso, Col. Lindavista, C.P 07738, Ciudad de México, México.

ABSTRACT
The present paper presents a theoretical analysis that corresponds to a second part of a complete investigation about the thermal influence on airfoil hydrodynamic boundary layer. The thermal influence on boundary layer of an aerodynamic airfoil surface is investigated in this thesis. Pressure, temperature and velocity conditions were considered from the 12th stage of axial compressor of a gas turbine RUSTOM TB-5000. A series of numerical simulations were performed using the Spalart-Allmaras model of turbulence. The inlet flow direction and the surface temperature were varied. The results of the simulations are shown by maps of distribution, in order to visualize the modification of the flow field in the area of step of the waterfall, and along the pressure and suction side of the blade. Perpendicular lines for monitoring the speed profiles and their modification due to the reduction of the temperature of the surface of the blade have been established.
The results show that the reduction of both the viscosity and the density of the gas produce a speed increase in the area near the wall within the boundary layer. As a consequence there is a reduction of boundary layer thickness up to 10.03% for a surface temperature of 410.9 K, and up to 17.80% with 310.9 K, compared to a surface with 510.9 K, this for the suction side with an angle of incidence of 15º. For the case of the pressure side of the blade, the greatest reduction in layer thickness limit is presented with an incidence angle of 0 to the cascade, up to 7.97% for 410.9 K and 17.73% for 310.9 K on the surface. Therefore, this phenomenon is more noticeable on the suction side of the blade, and increases with increasing angle incidence of the flow.
Keywords: *Thermal Influence, Airfoil, Hydrodynamic Boundary Layer, Numerical Simulation*

1. INTRODUCTION
Previously we presented a paper addressing the theoretical analysis part corresponding to a first part of a complete investigation about the thermal influence on airfoil hydrodynamic boundary layer. Compressor rotating stall was analyzed, specifically the principles of aerodynamics and airfoil stall, and rotating stall in compressor blading. Also, foundations on hydrodynamic boundary layer that include laminar and turbulent boundary layer, boundary layers in airfoils and boundary separation were addressed. A theoretical analysis about thermal boundary layer and heat transfer was considered. Therefore, the basis presented was of great importance for the correct understanding and implementation of the last addressed topic that deals with a test case study where many numerical simulations are carried out.
In this paper we study the influence exerted by the reduction of temperature in the surface of a blade NACA 0012 immersed in a linear cascade, on the development of the hydrodynamic boundary layer, by means of a numerical simulation. Firstly, we will set a constant free-flow velocity value, varying the angle of incidence of the incoming fluid, in addition the temperature is modified to each angle, analyzing the impact of temperature gradients on the development of boundary layer flow, monitoring the variations within the velocity profiles on the pressure side and suction of the airfoil, as well as the benefits that are generated.

2. TEMPERATURE, PRESSURE AND VELOCITY MAPS
According to the test cases presented before, 12 cases have been established to simulate, in which only two parameters have been modified, the angle of incidence of the fluid on the airfoil and the surface temperature of the blade. The numerical evaluation of all the cases was carried out and the

results will be presented together with the respective analysis.

Figure 1 shows the velocity distribution with a flow at 0 ° (angle of incidence in the cascade). In

Figure 1a, there are three zones that can be differentiated, the former is located anterior to the linear cascade of blades, presenting a constant distribution of the properties shown; the second zone presents a greater variation due to its location in the zone of passage between the blades, where there is a reduction of area; and the third is in the area behind the cascade of blades, in which the flow trail is developed due to the blades. In Figure 1b, two important areas in the development of flow on the airfoil have been highlighted, the area around the stagnation point where the dynamic pressure varies from a free stream value to zero at the stagnation point where the static pressure is equal to the total pressure. The flow wake zone is located posterior to the blade, where the flow develops at a slower speed due to the friction that exists with the surface of the body.

The analysis will focus in general on the passage area, the cascade of blades, and punctually, in the region surrounding the middle blade of the cascade, where the boundary layer develops. The patterns in the distribution of temperature, pressure and velocity will vary significantly depending on the angle of incidence of the flow on the cascade. In order to analyze the influence of the variation of the temperature of the airfoil surface on the development of the boundary layer, the results obtained will be compared to a determined angle, with only the surface airfoil temperature being varied.

According to the numerical simulations, the most relevant case for the evaluation of the thermal influence on the hydrodynamic boundary layer is in which the angle of flow incidence is 15 ° with respect to the direction of the airfoil chord.

Figure 2 shows the temperature distribution obtained at an angle of incidence of 15 ° at a blade surface temperature of 510.9K (figure a), 410.9K (figure b) and 310.9K (figure c). It is possible to see changes in the temperature distribution in the area of the flow wake zone, around the stagnation point, as well as in the front side of the blade suction side.

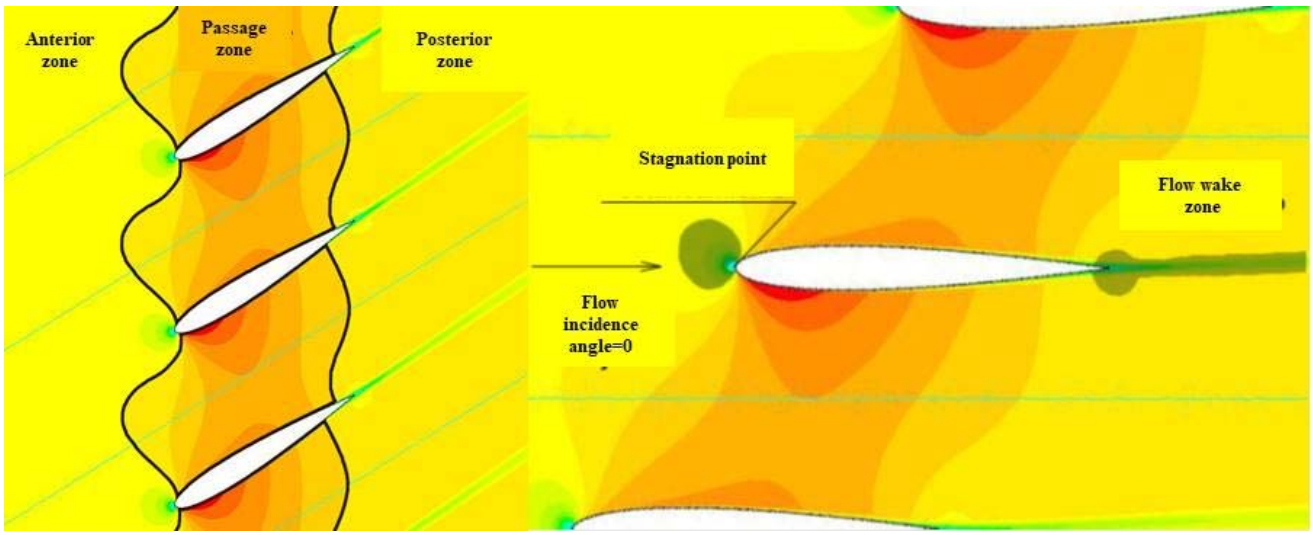

Figure 1 Zones around the blade in the cascade with a flow incidence of 0.

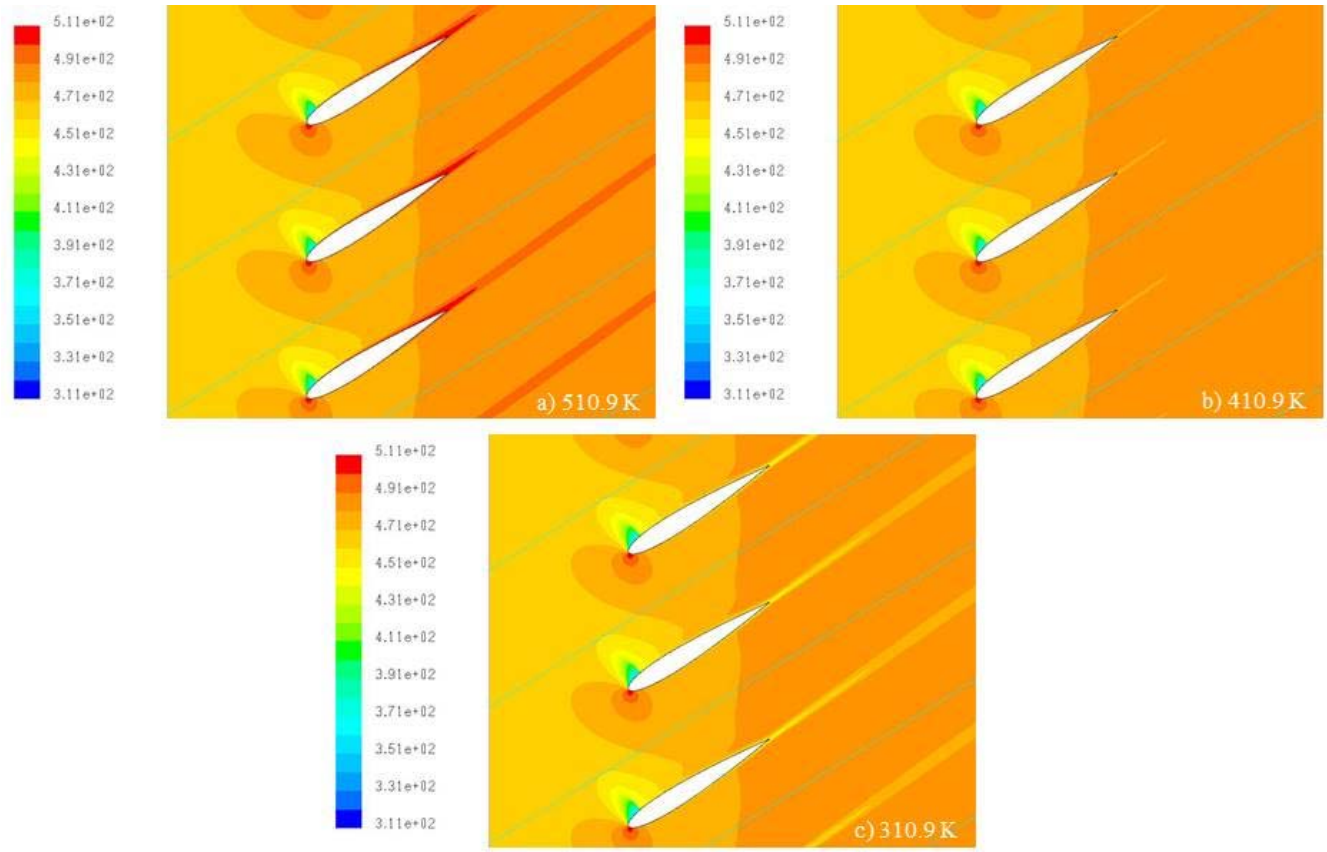

Figure 2. Temperature maps with incidence flow angle of 15º

In order to have a better appreciation of the changes in the temperature fields due to the reduction of 100K and 200K on the surface, the distribution maps of 510.9K and 410.9K have been superimposed, highlighting with gray the areas presenting a displacement in the value of the local temperature around the central blade, also the maps of 510.9K and 310.9K. This is shown in Figures 3 and 4. This action is performed for the distribution maps of dynamic viscosity, static pressure and velocity respectively. Figure 3 shows the effect of the 100K reduction on the surface temperature of the airfoil, revealing, first of all, a decrease in temperature in the area close to the airfoil surface that affects the rest of the distribution in the area of passage, highlighting the area around the stagnation point, the front part of the airfoil suction side and the development of the wake. The effect of the 200K reduction is shown in Figure 4 and has the same temperature reduction pattern as Figure 3, only with a larger area magnitude. This modification of the temperature distribution produces a variation in the magnitude of air properties, since the temperature is inversely bound to the dynamic viscosity, which is an important property in the fluid. From the above, it is possible to deduce that in the areas where there is a reduction of temperature, a reduction in the value of the dynamic viscosity will be presented. This phenomenon is observed in Figure 5 where the gray areas show the modification of the local value of the dynamic viscosity obtained by using a reduction of the surface temperature of the blade from 510.9K to 410.9K. When the surface temperature is reduced by 200K, as shown in Figure 6, the location of the areas where the dynamic viscosity value is altered is increased, increasing the area of reduction compared to the case where it is reduced by only 100K, being more noticeable this variation in the area near the blade and in the development of the flow wake. Such a reduction in temperature and dynamic viscosity in such zones results in an increase in the local velocity of the fluid as can be seen in Figures 7 and 8, in which the influence of the cooling of the surface in 100K and 200K respectively is observed. In turn, if the total

constant pressure is considered, the increase in velocity that is directly associated with the kinetic energy or dynamic pressure will affect the local static pressure inversely, so that a static pressure reduction will be obtained in the zones where the fluid is accelerated, this is depicted in Figures 9 and 10.

Another important property of the air that is affected is the density, since it is directly related to the static pressure and inverse to the temperature. For this case, both the static pressure and the temperature decrease, but since the increase in pressure is much greater than the decrease in temperature, the density will decrease. This effect will also help the local velocity of the fluid to increase, due to the increase in the specific volume of the gas.

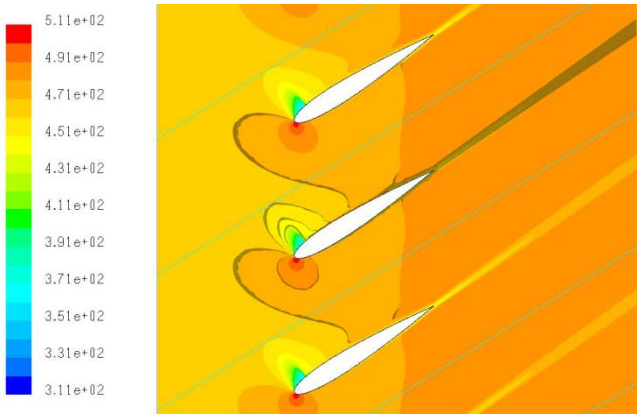

Figure 3. Variation of flow temperature profile (K) in the cascade due to the reduction of temperature on the airfoil surface (from 510.9 K to 410.9 K).

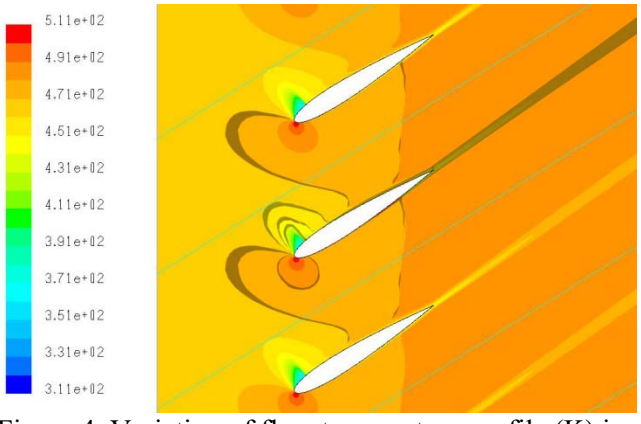

Figure 4. Variation of flow temperature profile (K) in the cascade due to the reduction of temperature on the airfoil surface (from 510.9 K to 310.9 K).

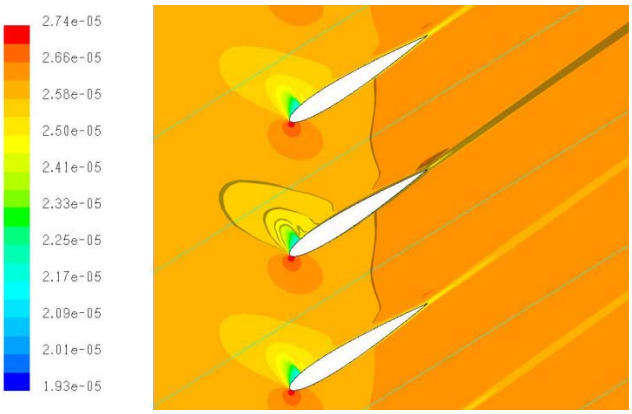

Figure 5. Variation of dynamic flow viscosity profile (Kg/m-s) in the cascade due to the reduction of temperature on the airfoil surface (from 510.9 K to 410.9 K).

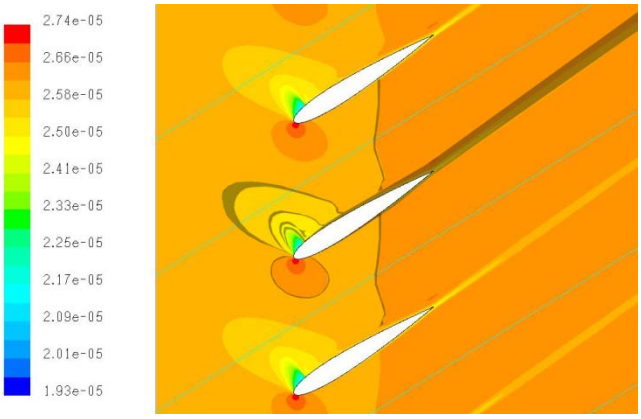

Figure 6. Variation of dynamic flow viscosity profile (Kg/m-s) in the cascade due to the reduction of temperature on the airfoil surface (from 510.9 K to 310.9 K).

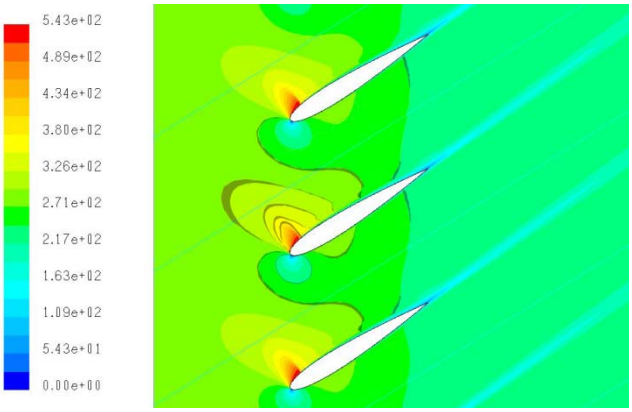

Figure 7. Variation of flow velocity profile (m/s) in the cascade due to the reduction of temperature on the airfoil surface (from 510.9 K to 410.9 K).

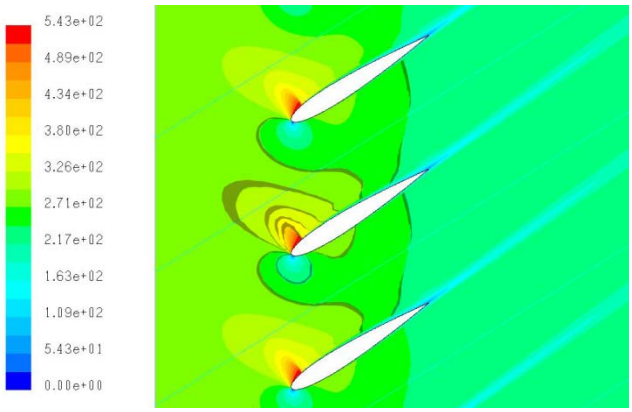

Figure 8. Variation of flow velocity profile (m/s) in the cascade due to the reduction of temperature on the airfoil surface (from 510.9 K to 310.9 K).

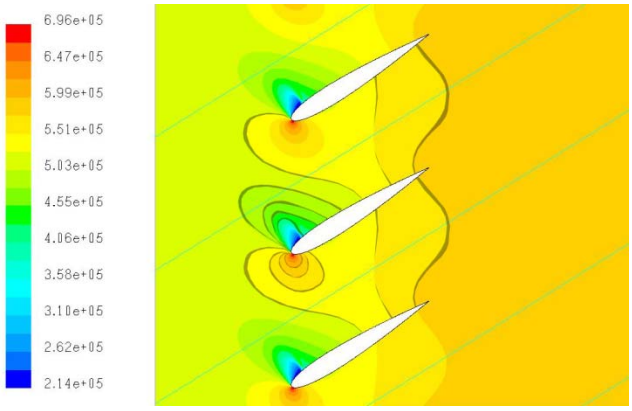

Figure 9. Variation of static pressure profile (Pa) in the cascade due to the reduction of temperature on the airfoil surface (from 510.9 K to 410.9 K).

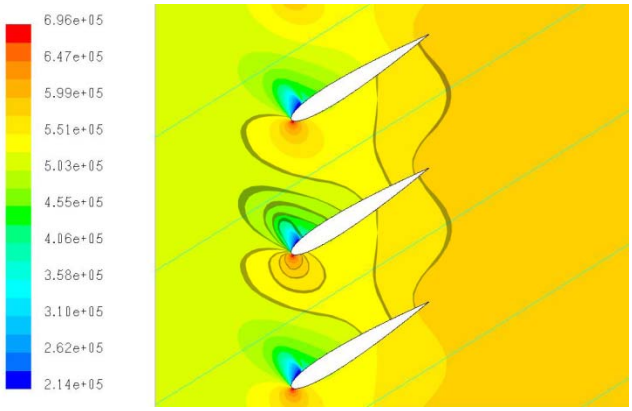

Figure 10. Variation of static pressure profile (Pa) in the cascade due to the reduction of temperature on the airfoil surface from 510.9 K to 310.9 K.

The reduction in temperature on the blade surface will positively affect not only the flow around the blade but also all of the rest of the fluid that crosses the blading. The cases in which the angle of incidence is 0º, 5º and 10º will not be presented in detail because the same tendency of the 15º case was showed, only with a smaller impact on the modification of the operating conditions and the physical properties of the air.

3. VELOCITY PROFILES AROUND THE NACA 0012

Twenty four lines of monitoring have been established along the entire surface of the blade, in order to know the development of the flow around it, 12 suction side monitoring lines and 12 pressure side lines. These lines are positioned at 2.5%, 5.0% and from 10.0% to 100% of the value of the blade chord. The graphs that will show the velocity profile have the dimensionless value u/U on the axis of the ordinates, and the graphs of the temperature profile the relation T/T_O, both profiles will express in the axis of the abscissa the value of the perpendicular distance to the surface. It is important to mention that the free stream velocity will not be the same for all monitoring points, due to the transformation of flow, kinetic and thermal energy working energies along the curved surface of the blade.

Figures 11 and 12 show the range of velocity profiles that runs along the blade pressure side for an angle of incidence of 0 °. The velocity profiles developed in the first 20.0% of the value of the string have a parabolic behavior, in which the effects of viscosity are very appreciable, because a low Reynolds number value is present in this zone. With the increase in the distance traveled by the fluid over the profile, the Reynolds number increases, modifying the velocity profile to the characteristic logarithmic type of fluids with high Reynolds number, as shown by the 60.0% of the chord in Figure 12. Up to 20.0% of the chord we have profiles in which it is not possible to distinguish the thermal influence on some of the lines presented, this is because in this zone the development of the boundary layer is still small, being this notorious difference from the 30.0% of the chord, where the difference is accentuated with

respect to the increase of the percentage of the chord. The velocity profiles presented on the pressure side of the blade at 510.9 K and 410.9 K of temperature are greater than those developed on a surface with 310.9 K of temperature; this indicates that there is an increase in the speed value produced by the reduction of temperature.

It is possible to see in a general way that the difference between the velocity profiles developed with a surface temperature of 510.9 K, 410.9 K and 310.9 K increases with the increase of the percentage of the chord, and with the increase of the length traveled by the fluid, the values of the Reynolds number are larger, which implies that the flow tends to be less ordered. The velocity varies in various proportions within the boundary layer due to the reduction of the surface temperature of the blade. The velocity profiles developed at 30.0% of the value of the chord with a surface at 410.9 K show an increment in the gradual velocity that goes from 23.0% at the beginning of the profile development to 0.64% at the end of the boundary layer, in relation to the profile developed at 510.9 K. For the case of 310.9 K, the increment of the gradual velocity goes from 58.0% at the beginning, to 1.34% at the end of the boundary layer. The velocity profiles developed at 90.0% of the chord value with a surface at 410.9 K show an incremental velocity increase from 25.9% at the beginning of the profile development to 0.80% at the end of the boundary layer, this in relation to the profile developed at 510.9 K. For the case of 310.9 K, the increment of the gradual speed goes from 63.4% at the beginning, to 1.75% at the end of the boundary layer. Figures 13 and 14 show the case with an incidence angle of 15º in the blade, corroborating the behavior trend mentioned previously in the velocity profiles, and in a general way they present the same behavior as the previous case.

Figures 15 and 16 show the profiles developed on the suction side of the blade with an angle of incidence of 0º. In the same way as on the pressure side, the first 20% of the chord has a velocity profile where the viscous effects are very appreciable because the ratio of inertial forces of the fluid to the viscous forces is very small. With the advance of the fluid on the surface of the body, the forces of inertia increase, modifying the velocity profile from 30% of the blade chord. In the same way as the pressure side, the difference between the velocity profiles developed with the three surface temperatures used becomes greater, as the percentage of the chord increases. As it is possible to observe in Figures 17 and 18, the difference between velocity profiles that develop in a same section of the surface of the suction side increases proportionally with the angle of incidence, contrary to the pressure side. An important aspect to remember is that the flow that develops along the suction surface becomes unstable with the increase in the angle of incidence of the fluid, to the point of presenting adverse pressure gradients that initiate the boundary layer separation. As mentioned before, there is a critical flow angle of incidence over the blade. If this angle is exceeded, flow separation is generated (Stall) producing a blockage phenomenon. For the NACA 0012 profile, the critical angle is 12º, although this depends on the conditions in which the flow is submerged.

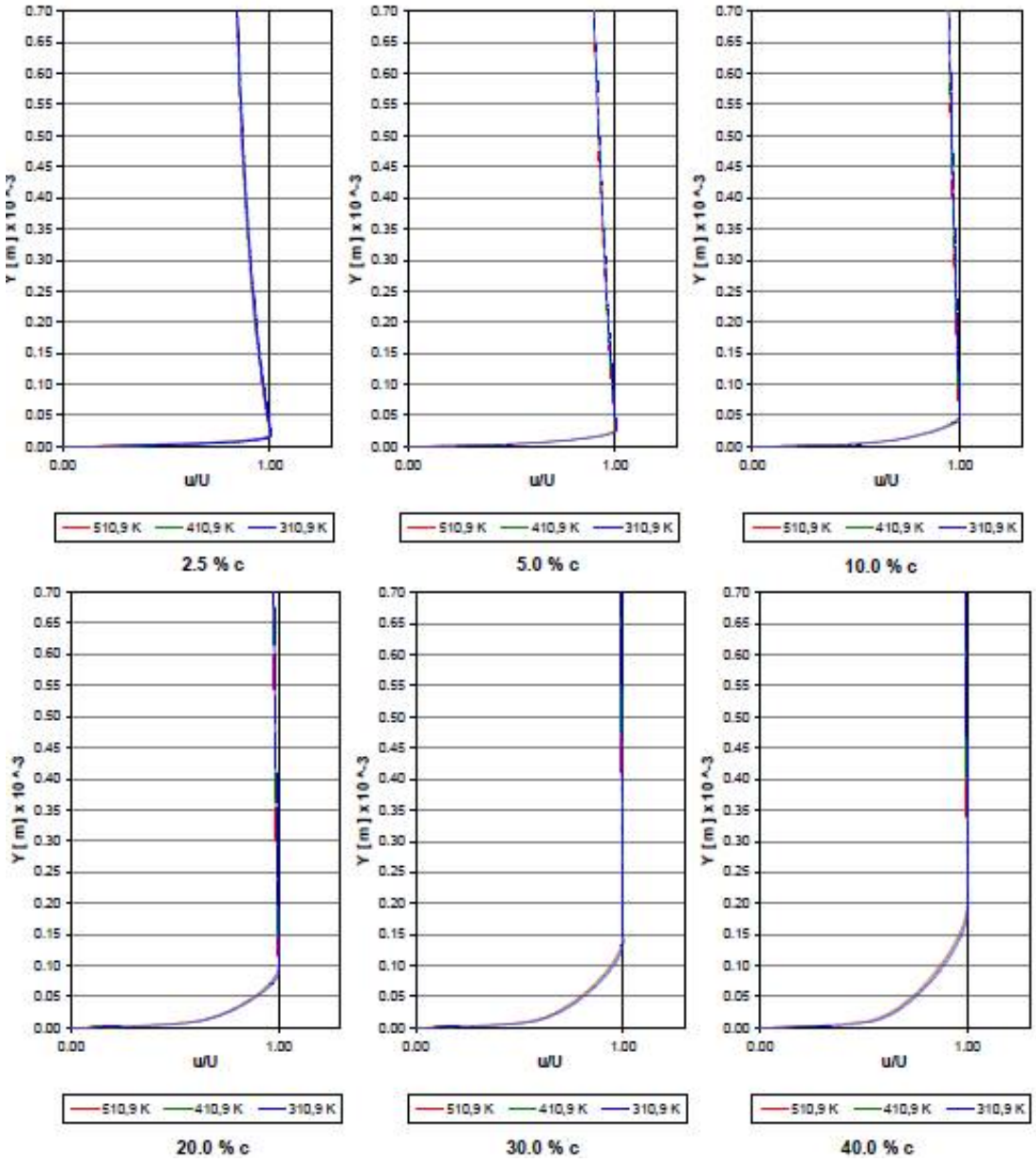

Figure 11. Velocity profiles with angle of incidence of 0º in the pressure side.

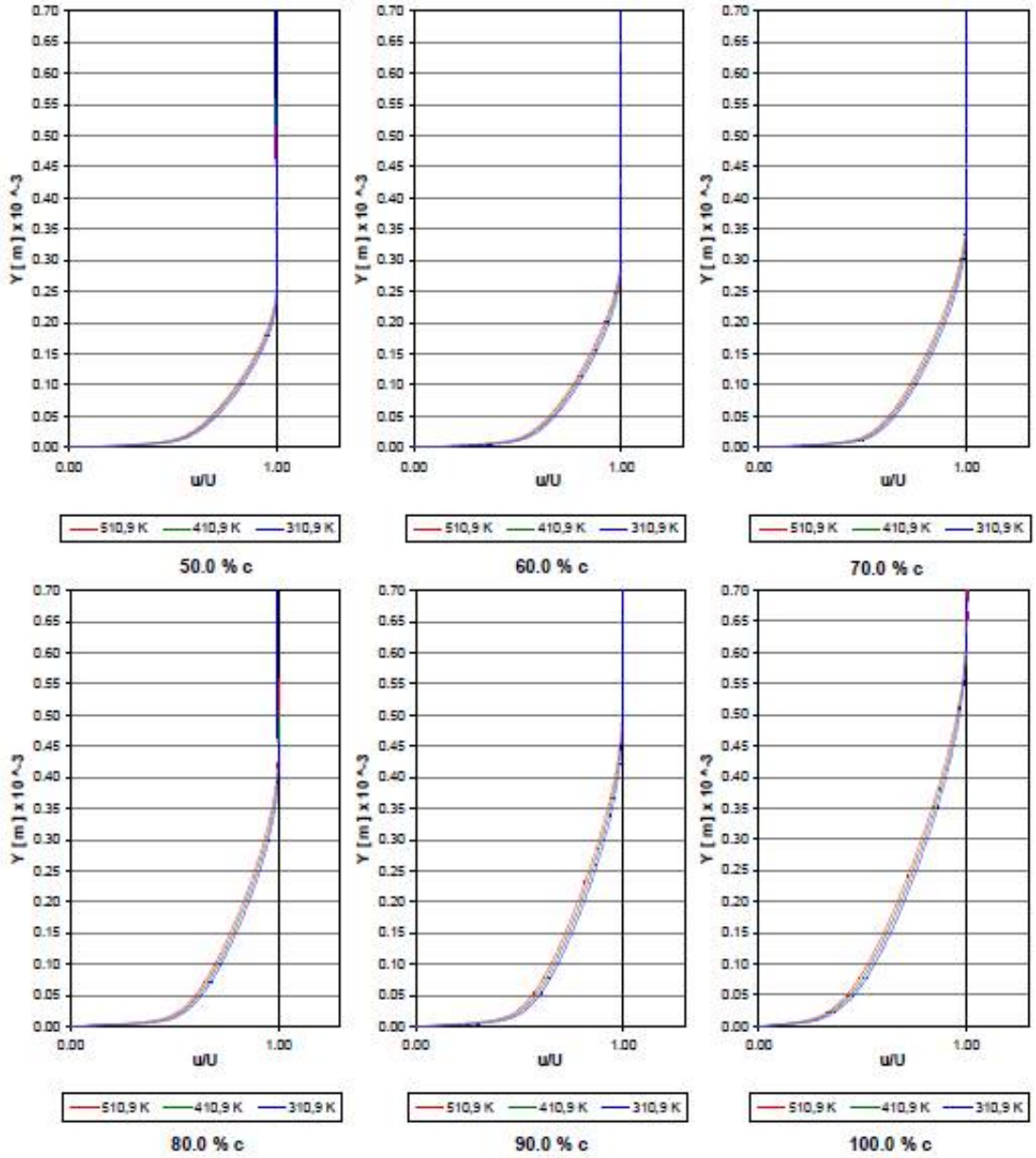

Figure 12. Velocity profiles with angle of incidence of 0º in the pressure side (Continuation).

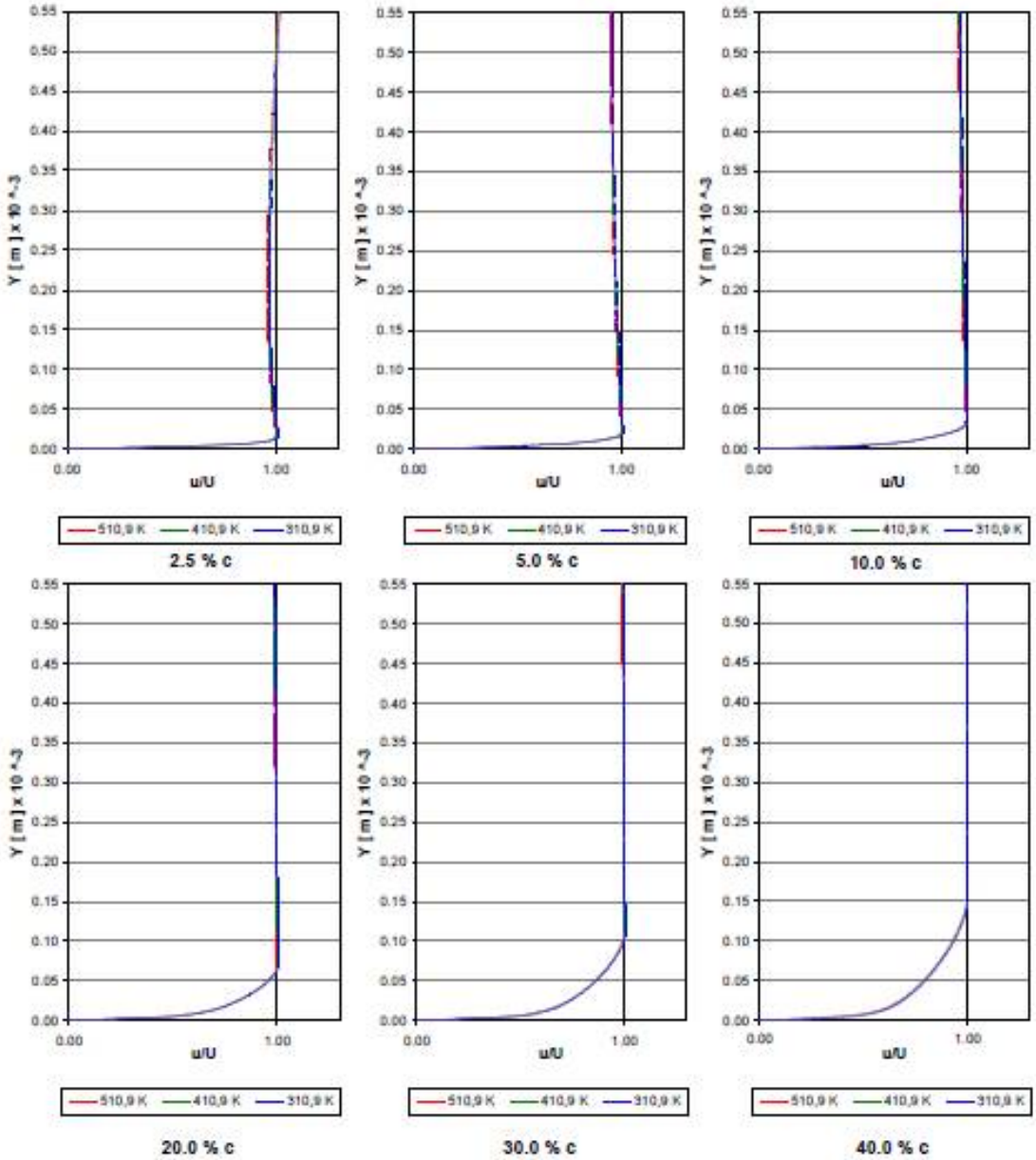

Figure 13. Velocity profiles with angle of incidence of 15º in the pressure side.

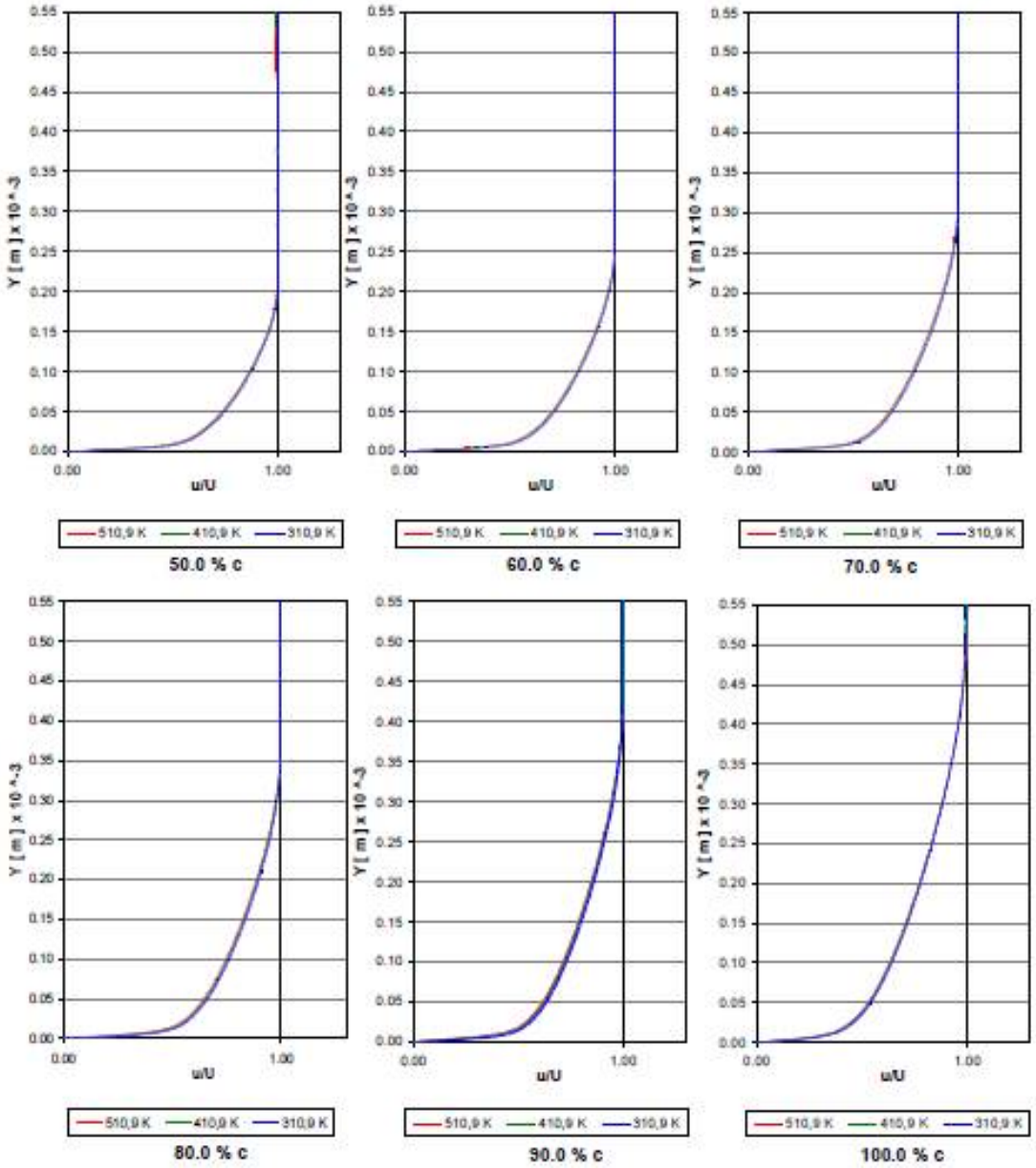

Figure 14. Velocity profiles with angle of incidence of 15º in the pressure side (Continuation).

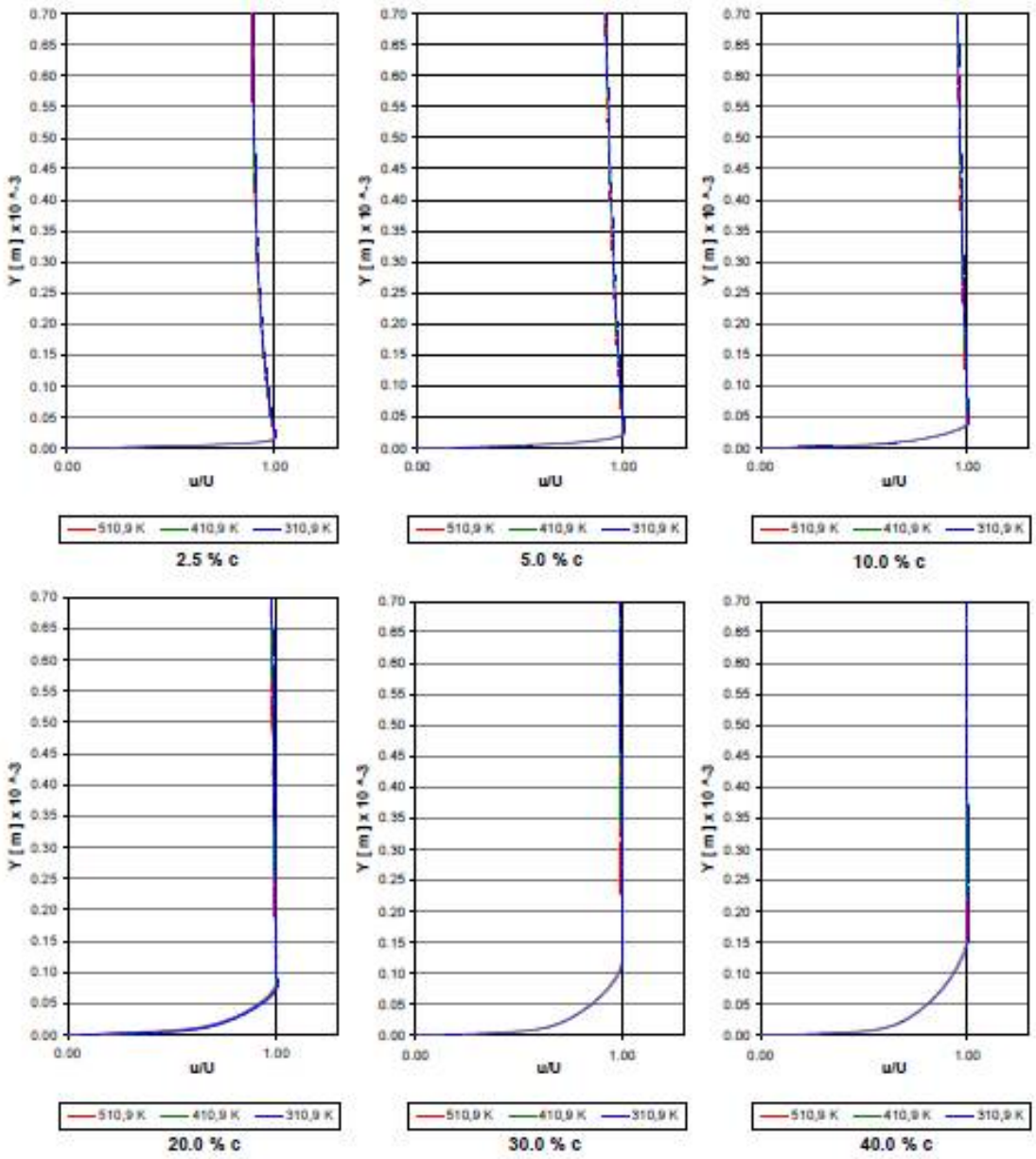

Figure 15. Velocity profiles with angle of incidence of 0º in the suction side.

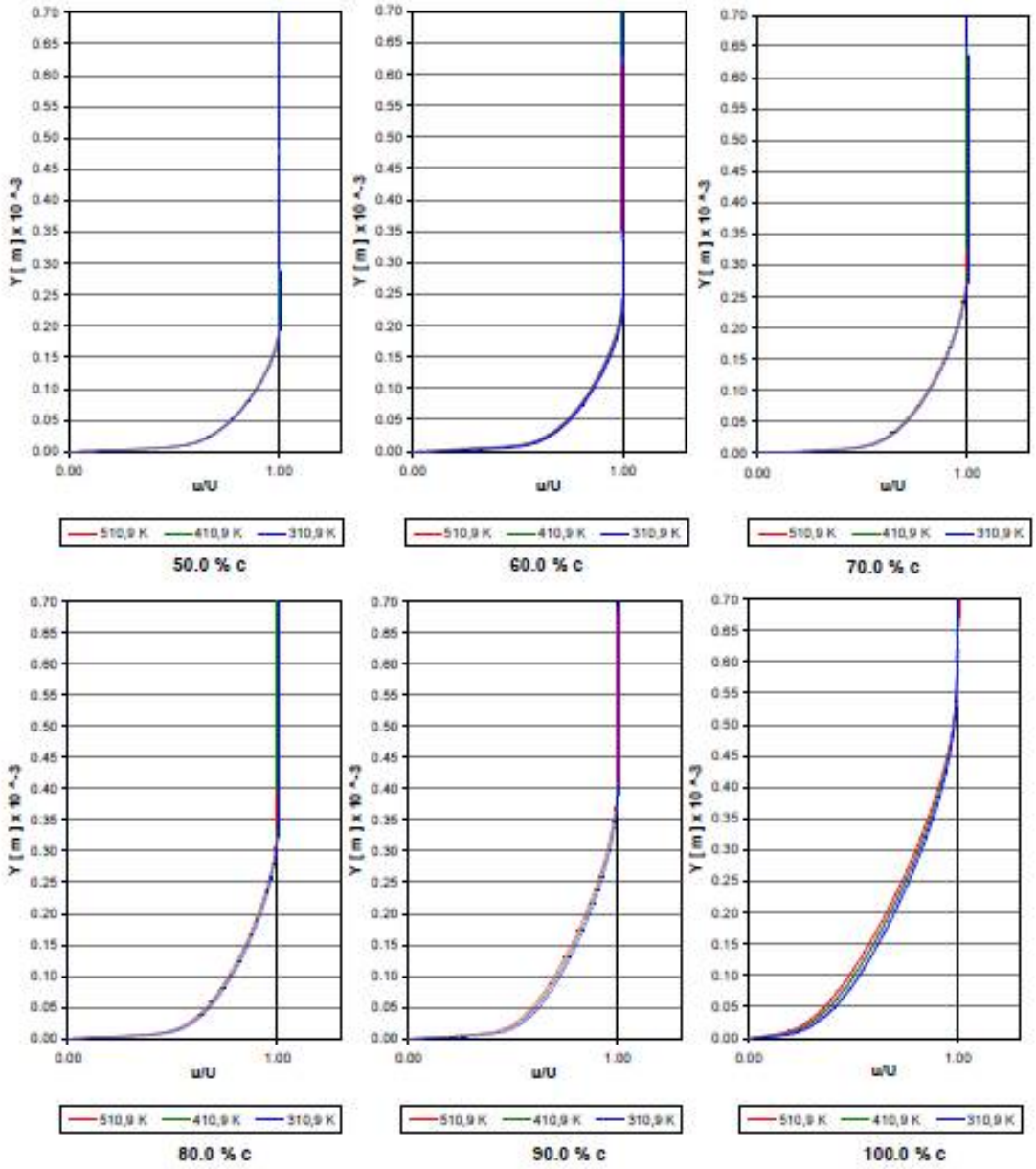

Figure 16. Velocity profiles with angle of incidence of 0º in the suction side (Continuation).

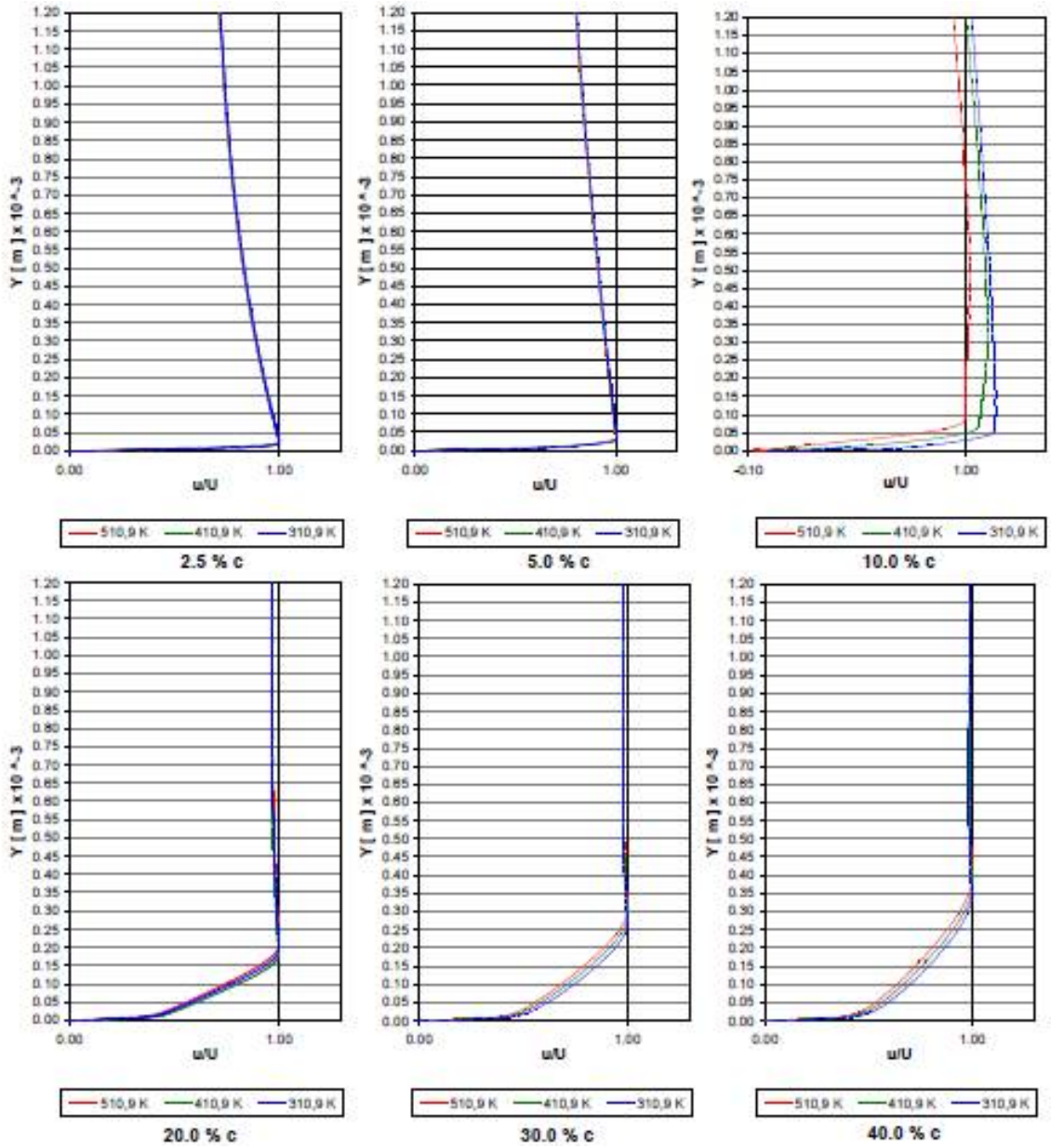

Figure 17. Velocity profiles with angle of incidence of 15º in the suction side.

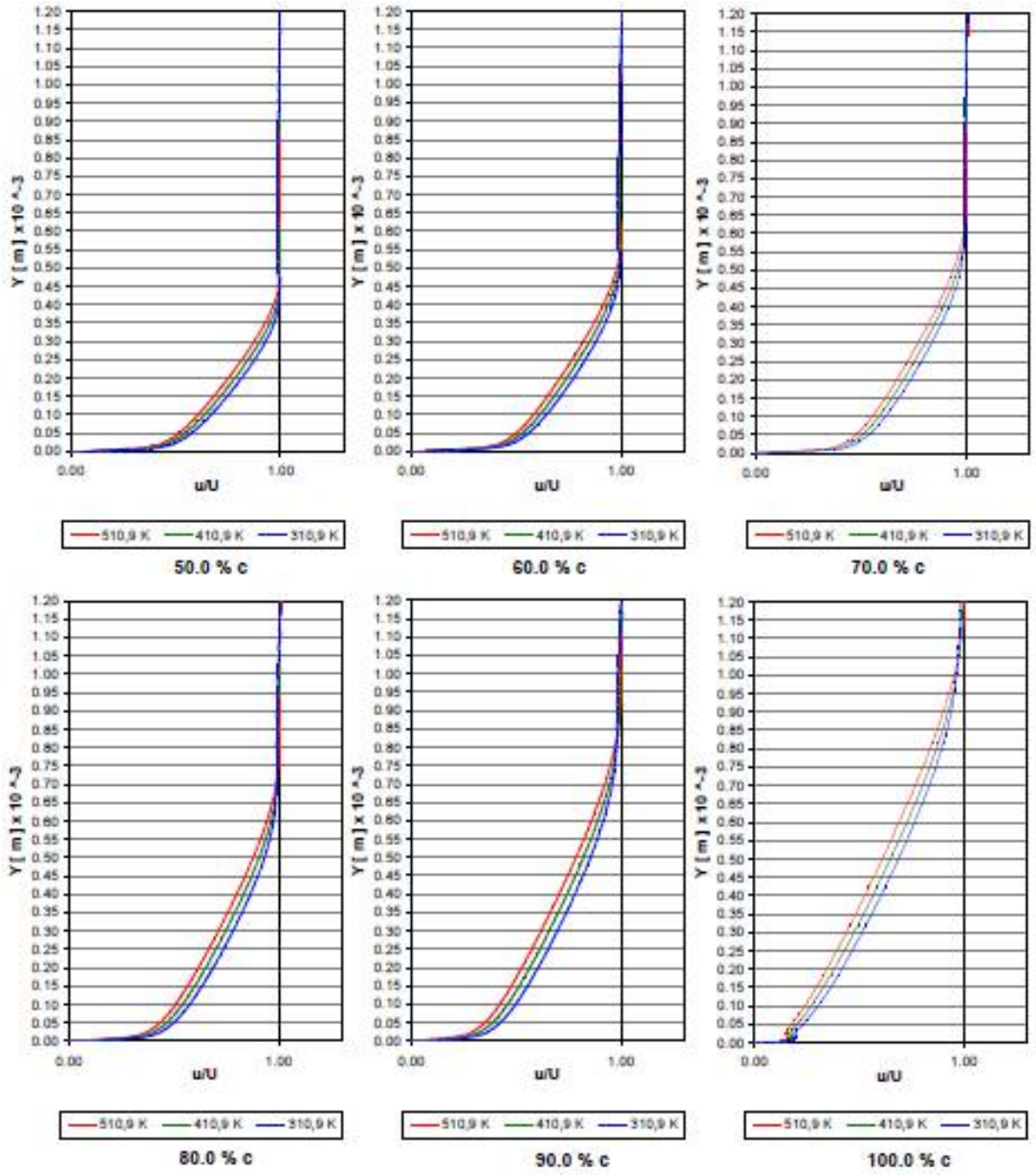

Figure 18. Velocity profiles with angle of incidence of 15º in the suction side (Continuation).

4. THERMAL AND HYDRODYNAMIC LIMIT LAYER

Figures show the growth of the thermal and hydrodynamic boundary layers, which is on the pressure side of the blade. It can be seen in the development of both layers, that the thickness is reduced with the increase of the angle of incidence of flow in the blade. In addition, the difference between the boundary layer generated with the different temperatures on the surface is also reduced. In the case of the suction side, this phenomenon is reversed, and the thermal and hydrodynamic boundary layers show a similar behavior between them. With the increase of the angle of attack to the entrance of the blade, the difference between the developed boundary layer thicknesses becomes greater, and the thickness itself grows.

The above can be easily verified in Tables 1 and 2, where we present the percentage of decrease of the hydrodynamic boundary layer on the pressure and suction side of the cases in which the cooling of the surface of the blade maintains a temperature of 410.9 K and 310.9 K, with respect to the case of 510.9 K.

It can be observed in the case in which the fluid enters the blading with an angle of 15º, there is an important alteration of the growth trend of the hydrodynamic and thermal boundary layer in the area from 9.0% to 11.0%. In the hydrodynamic boundary layer there is a sudden significant increase in thickness. This is attributed to the detachment of the boundary layer produced by the presence of an adverse pressure gradient, which breaks the equilibrium shown in the previous cases. In the case of the angle of attack of 15º, a reduction of the thickness of the boundary layer is shown of 15.85% for the surface to 310.9 K and 6.61% to 410.9 K in the 12.0% of the chord. In the posterior zone, there is a decrease between 3.33% and 10.03% for 410.9 K and 9.70% to 17.80% for 310.9 K, this on the suction side of the blade.

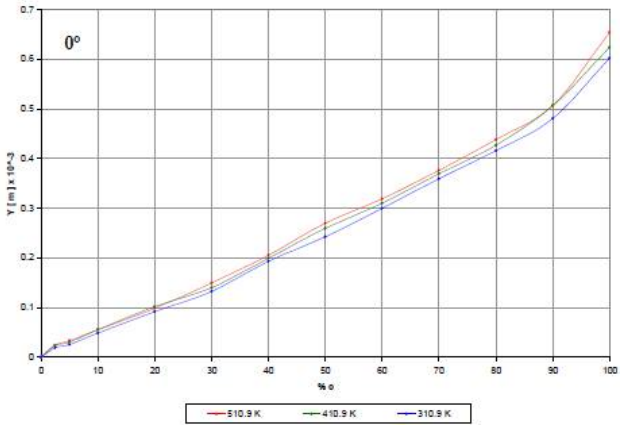

Figure 19. Thickness of the thermal boundary layer on the pressure side of the blade (with angle of incidence of 0º)

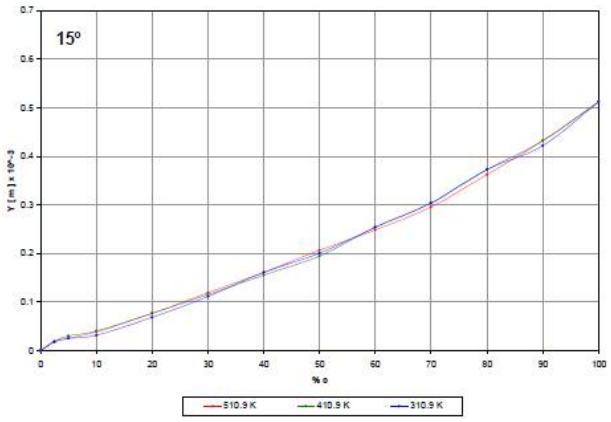

Figure 20. Thickness of the thermal boundary layer on the pressure side of the blade (with angle of incidence of 15º)

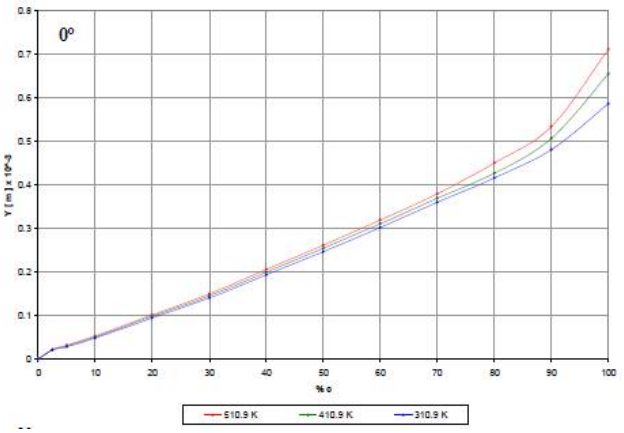

Figure 21. Thickness of the hydrodynamic boundary layer on the pressure side of the blade (with angle of incidence of 0º)

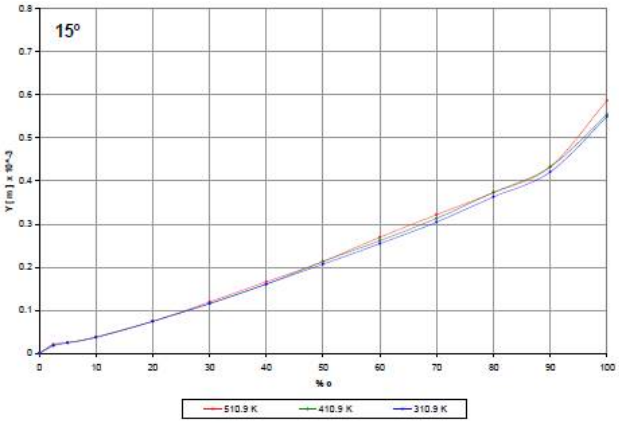

Figure 22. Thickness of the hydrodynamic boundary layer on the pressure side of the blade (with angle of incidence of 15º)

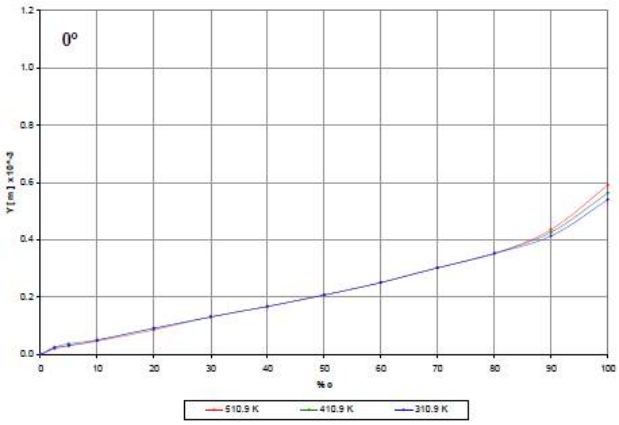

Figure 23. Thickness of the thermal boundary layer on the suction side of the blade (with angle of incidence of 0º)

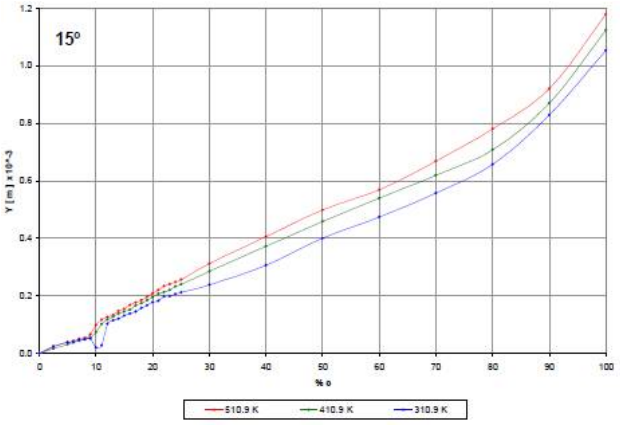

Figure 24. Thickness of the thermal boundary layer on the suction side of the blade (with angle of incidence of 15º)

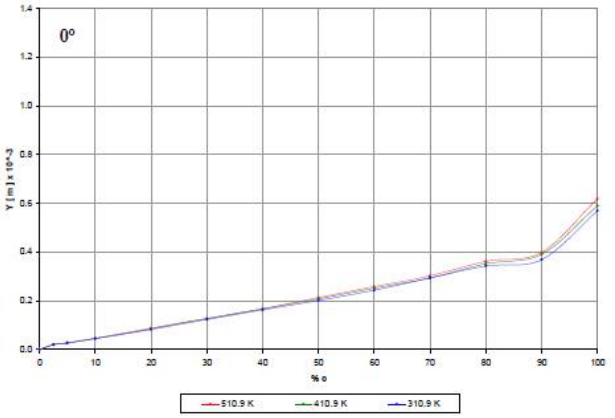

Figure 25. Thickness of the hydrodynamic boundary layer on the suction side of the blade (with angle of incidence of 0º)

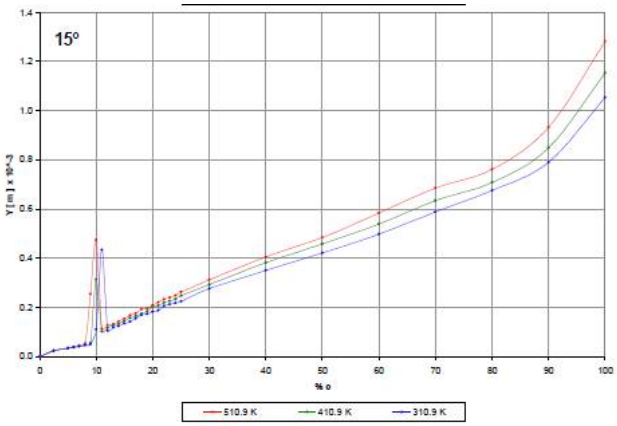

Figure 26. Thickness of the hydrodynamic boundary layer on the suction side of the blade (with angle of incidence of 15º)

Table 1. Percentage of reduction of the hydrodynamic boundary layer thickness of the pressure side of the blade, with respect to the case thickness for 510.9 K

% c	Angle of attack			
	0º		15º	
	410.9 K	310.9 K	410.9 K	310.9 K
	[%]	[%]	[%]	[%]
0	**0.00**	**0.00**	**0.00**	**0.00**
2.5	**6.44**	**6.44**	**6.67**	**13.13**
5.0	**5.35**	**10.52**	**0.00**	**5.88**
10.0	**4.23**	**8.34**	**0.00**	**4.77**
20.0	**3.41**	**6.71**	**0.00**	**0.00**
30.0	**3.16**	**6.23**	**3.25**	**3.25**
40.0	**3.00**	**5.92**	**3.06**	**3.06**
50.0	**2.88**	**5.68**	**0.00**	**2.94**
60.0	**2.78**	**5.48**	**2.83**	**5.59**
70.0	**2.70**	**5.34**	**2.76**	**5.46**
80.0	**5.20**	**7.70**	**0.00**	**2.71**
90.0	**5.06**	**9.90**	**0.00**	**2.65**
100.0	**7.97**	**17.63**	**5.35**	**6.38**

Table 2. Percentage of reduction of the hydrodynamic boundary layer thickness of the suction side of the blade, with respect to the case thickness for 510.9 K

Angle of attack= 15º								
% c	410.9 K [%]	310.9 K [%]	% c	410.9 K [%]	310.9 K [%]	% c	410.9 K [%]	310.9 K [%]
0	**0.00**	**0.00**	14.0	**6.48**	**12.58**	25.0	**5.99**	**14.36**
2.5	**0.00**	**5.70**	15.0	**6.40**	**12.43**	30.0	**5.85**	**11.39**
5.0	**4.75**	**4.75**	16.0	**6.33**	**15.15**	40.0	**5.84**	**13.42**
6.0	**4.60**	**4.60**	17.0	**6.28**	**12.21**	50.0	**5.34**	**12.85**
7.0	**4.47**	**4.47**	18.0	**9.19**	**12.08**	60.0	**7.57**	**14.61**
8.0	**8.48**	**12.51**	19.0	**6.20**	**12.04**	70.0	**7.29**	**14.09**
9.0	**77.85**	**80.06**	20.0	**3.12**	**11.97**	80.0	**7.07**	**11.26**
10.0	**33.80**	**76.74**	21.0	**6.12**	**14.66**	90.0	**8.96**	**15.22**
11.0	**9.99**	**-282.97**	22.0	**6.08**	**11.82**	100.0	**10.03**	**17.80**
12.0	**6.61**	**15.85**	23.0	**6.05**	**11.77**			
13.0	**3.33**	**9.70**	24.0	**6.03**	**11.72**			

CONCLUSIONS

Numerical results, such velocity, pressure and temperature fields have been showed to look at the influence of cooling airfoil surface to flow of fluid through the cascade blade and around the pressure and suction blade side. Perpendicular monitoring lines to evaluate velocity profiles modification were placed on both pressure and suction surface. Air viscosity and density reduction produce an increase of the fluid velocity near the wall within the boundary layer meanwhile deceleration take place due the airfoil sag and internal fluid friction. This probably moves the negative pressure gradient on the suction side 1% of the airfoil chord, when the input angle is 15º and the surface temperature goes from 510.9K to 410.9K, and 2% when the temperature blade surface drops 200K.

As a consequence of the velocity increase inside of viscous area, a reduction of hydrodynamic boundary layer thickness is present. In the case when the input angle is 15º, the thickness reduction reaches 10.03% when the airfoil temperature is 410.9K and 17.8% with 310.9K in surface temperature, these found in suction blade side. In the case of pressure blade side, the great thickness reduction was present when the input angle is 0º with respect of airfoil chord, 7.97% with a surface temperature of 410.9K and 17.73% and airfoil temperature of 310.9K.

The difference between velocity profiles is increased when the input angle increase on the suction side of the airfoil while the same difference decreases on the pressure side at the same time. The numerical simulations shows that reducing surface temperature produces a better effects on surface zones of less stable flow as suction blade side.

REFERENCES

[1] P. Boyce, Meherwan “Gas turbine engineering handbook”, Gulf Publishing Company, first edition, 1982, p 603

[2] W. R. Hawthorne “Aerodynamics of turbines and compressors” Board, first, 1964, p 616

[3] Greitzer, E. M., “The Stability of Pumping Systems,” J. Fluids Engineering, Vol.103, pp. 193-242, June 1981

[4] Emmons, H. W., Pearson, C. E., andGrant, H. P.,Compressor Surge and Stall Propagation, Trans. A. S. M. E.,77, 455–467 (1955).

[5] P. Incropera, Frank / P. De UIT, David “Introduction to Heat Transfer “ John Wiley &Sons, third edition, 1996, p 795

[6] Bejan, Adrian “ Convection heat transfer “, John Wiley & Sons, Inc., second edition, 1995, p 623

[7] Rodríguez Dávalos, Jesús “Recuperación de álabes del compresor de turbina de gas marca RUSTON modelo TB-5000” Report, PEMEX, 1999

[8]Jacobs, Eastman N., Ward, Kenneth E., and Pinkerton, Robert M.:“The Characteristics of 78 Related Airfoil Sections from Tests in the Variable density Wind Tunnel” NACA Rept. No. 460, 1932.

[9] Paciorri R., Dieudonné W., "Validation of the Spalart-Allmaras turbulence model for application in hypersonic flows", Von Karman Institute for fluid Dynamics, Sint-Genesius-Rode, Belgium, 1997

[10] Bardina J.E., Huang P.G., Coakley T.J., "Turbulence modeling validation, testing, y development" NASA Technical Memorandum 110446, National Aeronautics and Space Administration, 1997

[11] P. Spalart and S. Allmaras, "A one-equation turbulence model for aerodynamic flows" Technical Report AIAA-92-0439, American Institute of Aeronautics and Astronautics, 1992.